

## Residual Halide Groups in Gilch-Polymerized Poly(*p*-phenylene-vinylene) and Their Impact on Performance and Lifetime of Organic Light-Emitting Diodes

A. Fleissner,<sup>†</sup> K. Stegmaier,<sup>†</sup> C. Melzer,<sup>\*,†</sup> H. von Seggern,<sup>†</sup> T. Schwalm,<sup>‡</sup> and M. Rehahn<sup>‡</sup>

<sup>†</sup>*Institute of Materials Science, Electronic Materials Department, Darmstadt University of Technology Petersenstrasse 23, 64287 Darmstadt, Germany, and* <sup>‡</sup>*Ernst-Berl-Institute for Chemical Engineering and Macromolecular Science, Chemistry Department, Darmstadt University of Technology, Petersenstrasse 22, 64287 Darmstadt, Germany*

Received June 2, 2009. Revised Manuscript Received July 16, 2009

On the basis of new insights into the reaction mechanism of the so-called Gilch route leading to poly(*p*-phenylene-vinylene)s (PPVs), the importance of vinyl halide defects for the performance of organic light-emitting diodes (OLEDs) is stressed in the present contribution. It is found that the current density, the luminance, and luminance efficiency are superior for PPVs that were subject to a long-term dehydrohalogenation. In particular, the device lifetime improves by a factor of 200 as long as the halide content is reduced from 0.4 to 0.05 wt %. The results imply that rather the mentioned vinyl halide defect than the often discussed tolane-bisbenzyl (TBB) defect has to be considered when investigating lifetime and performance of OLEDs. The device behavior is analyzed in view of a detailed study of the charge-carrier transport properties. We suggest that the penetration of electrons from the cathode in the PPV leads to a separation of halogen and thus to free halogen anions. The anions can move in the electric field to the contacts where they form a salt with the counterion present in the electrode material. The charge-carrier transport across the respective contact is thus impeded as a consequence of the appearance of a salt-containing interlayer. The proposed mechanism explains the observed differences in device performance and lifetime.

### Introduction

Soluble poly(*p*-phenylene-vinylene) (PPV) derivatives are promising materials for organic light-emitting diodes (OLEDs) used in displays or lighting applications, and the Gilch route is one of the preferred ways for their preparation.<sup>1–5</sup> In contrast to small molecules, polymeric organic semiconductors such as PPV offer the advantage of solution processing and therefore render fabrication methods like inkjet printing possible.<sup>6</sup> On the other hand, the lifetime of polymer-based OLEDs is generally still below those comprised of small molecules.<sup>7</sup> To find appropriate measures for increasing the device lifetime of polymer-based OLEDs, it has been studied whether PPVs prepared by the usual Gilch procedure exhibit exceptionally critical constitutional defects within their

backbones, which induce the aging and fatiguing processes in the operating devices predominantly. In this respect, it is known that Gilch PPVs contain cis-configured ethynylene units, in the range of some few percents, in their otherwise trans-configured main chains (Figure 1).<sup>4,8,9</sup> Moreover, Becker et al. identified another characteristic defect, for which they coined the term tolane-bisbenzyl (TBB) defect.<sup>8</sup> This defect structure comprises a sequence of a phenylene ethynylene and a phenylene ethylene moiety instead of two regular phenylene vinylene repeating units (Figure 1). The fraction of regular phenylene vinylene groups replaced by TBB defects was estimated from NMR measurements as 3–4% in Gilch-polymerized poly[*p*-(2-methoxy-5-(3,7-dimethyloctyloxy)phenylene-vinylene)] (OC<sub>1</sub>C<sub>10</sub>).<sup>8</sup> Soon after identification of the TBB moiety, Becker et al. correlated a reduced amount of TBB defects with an increased lifetime of PPV-based OLEDs and thus stimulated a quest for finding Gilch PPVs with a low amount of TBB defects.<sup>10</sup> This aim was achieved by different research groups, who showed an influence of electron donating side groups,<sup>10</sup> careful choice of reaction

\*Corresponding author. E-mail: melzer@e-mat.tu-darmstadt.de.

- (1) Braun, D.; Heeger, A. J. *Appl. Phys. Lett.* **1991**, *58*, 1982.
- (2) Friend, R. H.; Gymer, R. W.; Holmes, A. B.; Burroughes, J. H.; Marks, R. N.; Taliani, C.; Bradley, D. D. C.; Dos Santos, D. A.; Bredas, J. L.; Logdlund, M.; Salaneck, W. R. *Nature* **1999**, *397*, 121.
- (3) Kraft, A.; Grimsdale, A. C.; Holmes, A. B. *Angew. Chem., Int. Ed.* **1998**, *37*, 402.
- (4) Schwalm, T.; Wiesecke, J.; Immel, S.; Rehahn, M. *Macromol. Rapid Commun.* **2009**, *30*, 1295.
- (5) Grimsdale, A. C.; Chan, K. L.; Martin, R. E.; Jokisz, P. G.; Holmes, A. B. *Chem. Rev.* **2009**, *897*–1091.
- (6) Forrest, S. R. *Nature* **2004**, *428*, 911.
- (7) Hertel, D.; Müller, C. D.; Meerhold, K. *Chem. Unserer Zeit* **2005**, *39*, 336.

- (8) Becker, H.; Spreitzer, H.; Ibrom, K.; Kreuder, W. *Macromolecules* **1999**, *32*, 4925.
- (9) Roex, H.; Adriaenssens, P.; Vanderzande, D.; Gelan, J. *Macromolecules* **2003**, *36*, 5613.
- (10) Becker, H.; Spreitzer, H.; Kreuder, W.; Kluge, E.; Schenk, H.; Parker, I.; Cao, Y. *Adv. Mater.* **2000**, *12*, 42.

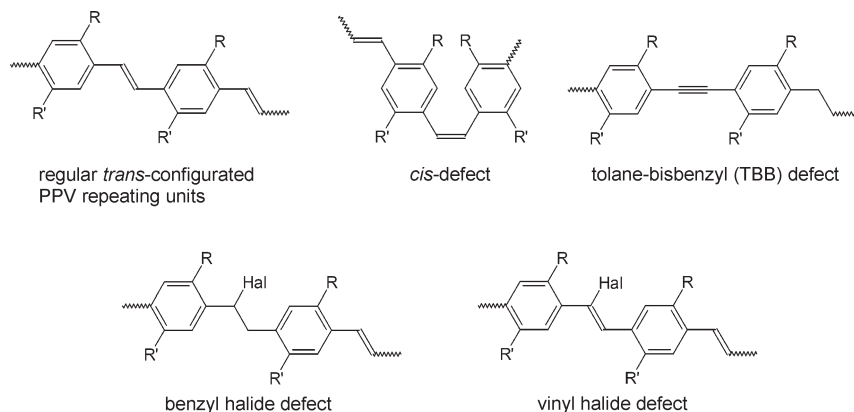


**Figure 1.** Regular PPV repeating units and four possible defect structures.

temperature,<sup>11</sup> steric hindrance induced by side groups,<sup>12</sup> and polarity of the solvent<sup>12</sup> on the amount of TBB defects. Currently, novel PPVs polymerized via the Gilch route are frequently characterized by their TBB content.<sup>13–15</sup>

In contrast, two other possible defects in Gilch-synthesized PPVs have attracted only little attention so far: incomplete dehydrohalogenation may lead to partially nonconjugated PPVs with remaining halogen in the backbone, resulting in a “benzyl halide” or a “vinyl halide” defect. These defects are shown in Figure 1 as well. From NMR measurements, Roex et al. found that approximately 3% of the repeating units in Gilch-polymerized OC<sub>1</sub>C<sub>10</sub> were affected by residual halogen.<sup>9</sup> They argued that this defect was not detected in the NMR studies of Becker et al.<sup>8</sup> because of different experimental conditions and a weaker signal-to-noise ratio. Johansson et al. showed that the amount of residual halogen decreases with increasing reaction temperature for poly[*p*-(2-(2,5-bis(2-ethylhexyloxy)phenyl)phenylene-vinylene)] (BEHP-PPV) prepared from monomers with a bromine leaving group, bromine contents of 0.58–4.4 wt % have been found for reaction temperatures between 0 °C and –78 °C and reaction times of 4 h.<sup>16</sup> Andersson et al. found traces of bromine in OC<sub>1</sub>C<sub>10</sub> and speculated that it might play an important role in the degradation of polymer OLEDs.<sup>17</sup> However, neither did they verify this claim experimentally, nor did they provide an explanation for the origin of the bromine. None of the aforementioned works studied the influence of the amount of uneliminated halogen groups on the lifetime of OLEDs. Moreover, none of

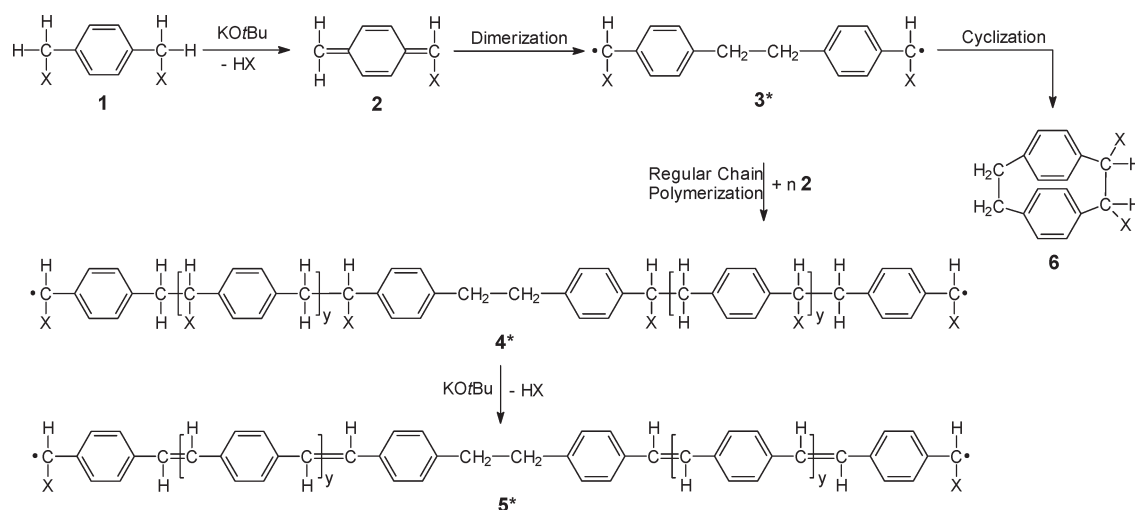
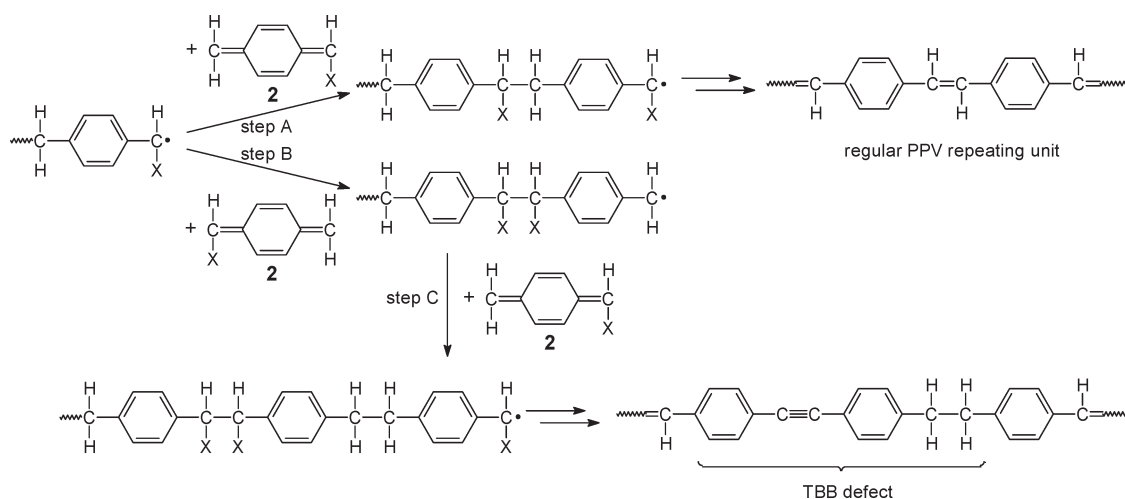
these studies took into consideration reasons for persisting halides, residing in the PPVs even over long reaction times, other than the already mentioned incomplete dehydrohalogenation of “regular” benzyl halide intermediates.

The distinct lack of literature relating the halide defects with the characteristics and lifetime of OLEDs based on Gilch-synthesized PPVs leaves the question of its importance for the performance of OLEDs unanswered. Especially, it remains unclear whether the degree of dehydrohalogenation that is achieved for common experimental conditions of the Gilch synthesis allows to rule out any influence of the residual halogen on the lifetime and performance of OLEDs that might interfere with studies that relate, for example, the TBB content with the lifetime. In this work, we show that halide defects indeed do have a strong effect on the lifetime and performance of OLEDs based on Gilch PPVs, and that the device lifetime and performance can be improved by decreasing this defect content. For this, we present a simple way for reducing the content of the defect during the Gilch synthesis of poly[*p*-(2,5-di(2-ethylhexyloxy)phenylene-vinylene)] (OC<sub>8</sub>C<sub>8</sub>). It will be argued that the constitution of the relevant halide defects differs from what has been discussed in the literature so far. We are able to pinpoint the drastic effect that halide has on the characteristics and lifetime of OLEDs, even if just fractions of a percent of the halogen groups remain uneliminated. Furthermore, we discuss how the halide defects affect the device characteristics, and finally, we propose a mechanism for the observed rapid failure of OLEDs with a high amount of such defects.

**Latest Knowledge about the Mechanism of the Gilch Reaction and Its Implications on Defects in PPV.** Recently, some of us reported the results of a detailed mechanistic reinvestigation of the Gilch synthesis of PPV.<sup>[4,18–24]</sup> The

- (11) Johansson, D. M.; Wang, X. J.; Johansson, T.; Inganäs, O.; Yu, G.; Srdanov, G.; Andersson, M. R. *Macromolecules* **2002**, *35*, 4997.
- (12) Chen, Z.-K.; Lee, N. H. S.; Huang, W.; Xu, Y. S.; Cao, Y. *Macromolecules* **2003**, *36*, 1009.
- (13) Huang, C.; Zhen, C.-G.; Su, S. P.; Vijila, C.; Balakrishnan, B.; Auch, M. D. J.; Loh, K. P.; Chen, Z.-K. *Polymer* **2006**, *47*, 1820.
- (14) Chang, H.-T.; Lee, H.-T.; Yeh, M.-Y. *J. Appl. Polym. Sci.* **2007**, *103*, 2743.
- (15) Chang, H.-T.; Lee, H.-T.; Chang, E.-C.; Yeh, M.-Y. *Polym. Eng. Sci.* **2007**, *47*, 1380.
- (16) Johansson, D. M.; Theander, M.; Srdanov, G.; Yu, G.; Inganäs, O.; Andersson, M. R. *Macromolecules* **2001**, *34*, 3716.
- (17) Andersson, G.; Brongersma, H. H.; Denier van der Gon, A. W.; van Ijzendoorn, L. J.; de Jong, M. P.; de Voigt, M. J. A. *Synth. Met.* **2000**, *113*, 245.

- (18) Schwalm, T.; Rehahn, M. *Macromol. Rapid Commun.* **2008**, *29*, 207.
- (19) Schwalm, T.; Rehahn, M. *Macromol. Rapid Commun.* **2008**, *29*, 33.
- (20) Schwalm, T.; Wiesecke, J.; Immel, S.; Rehahn, M. *Macromolecules* **2007**, *40*, 8842.
- (21) Schwalm, T.; Rehahn, M. *Macromolecules* **2007**, *40*, 3921.
- (22) Wiesecke, J.; Rehahn, M. *Macromol. Rapid Commun.* **2007**, *28*, 188.
- (23) Wiesecke, J.; Rehahn, M. *Macromol. Rapid Commun.* **2007**, *28*, 78.
- (24) Wiesecke, J.; Rehahn, M. *Angew. Chem., Int. Ed.* **2003**, *42*, 567.

**Scheme 1. Mechanism of the Gilch Synthesis of PPV (solubilizing side groups R, R' are omitted for clarity); X = Cl or Br, KOtBu = potassium *tert*-butanolate****Scheme 2. Formation of TBB defects in Gilch-Synthesized PPVs**

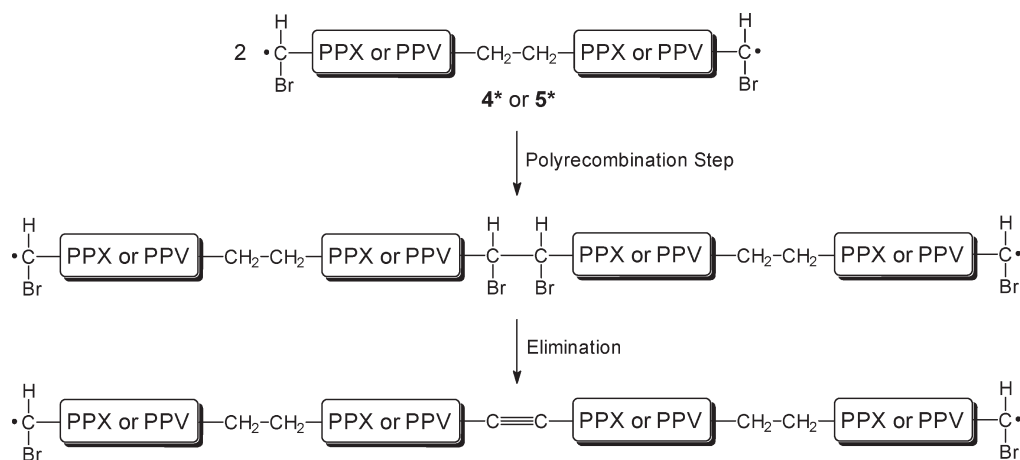
key conclusions are summarized in Scheme 1: it was shown that the first step in the reaction sequence is dehydrohalogenation of the usually applied starting material **1**, which leads to the real Gilch monomer, i.e.,  $\alpha$ -halo-*p*-quinodimethane **2**. Its subsequent polymerization is induced by diradicals **3\***, which form via spontaneous dimerization of some few *p*-quinodimethane molecules **2**. This is a rather surprising reaction, however, it is observed even at temperatures of below  $-60^\circ\text{C}$ . Some of the resulting diradicals **3\*** undergo intramolecular recombination, leading to *p*-cyclophanes such as **6**, which are the characteristic side products of Gilch polymerizations. All other diradicals **3\*** start regular chain growth which, *nota bene*, proceeds via macro-diradicals **4\***. Nearly simultaneously, the intermediately formed halide-containing PPX repeating units of **4\*** transform into those of PPV **5\*** via a second cascade of dehydrohalogenation steps.

The reaction mechanism shown in Scheme 1 has a number of implications with respect to the formation of defects within the PPVs. First of all, the initiation step itself creates the first defect: this is the CH<sub>2</sub>–CH<sub>2</sub> single bond in

the center of dimer diradical **3\***. Consequently, at least one defect that interrupts the  $\pi$ -electron conjugation is inherently present in any PPV chain. The well-known TBB defects, on the other hand, appear because of inverse monomer placements: usually, the chains grow via consecutive head-to-tail addition of monomers **2** to the radical chain ends (step A in Scheme 2). This monomer orientation is clearly preferred because of the much more efficient stabilization of the radical entity when located at the halide-bearing carbon, compared to that offered at the alternative CH<sub>2</sub> terminus.<sup>20,25</sup> From time to time, however, it happens that a monomer **2** is nevertheless attached in the opposite direction, i.e., via head–head placement (step B in Scheme 2), resulting in the formation of a CHX–CHX unit. Because of the rather inefficient stabilization of the thus formed CH<sub>2</sub>-centered radical, a regular next monomer addition step is the most likely event, leading back to the preferred CHX-centered radical (step C in Scheme 2), thereby causing a CH<sub>2</sub>–CH<sub>2</sub> moiety. When chain growth continues further, and after 2-fold dehydrohalogenation of

(25) Schwalm, T.; Immel, S.; Rehahn, M. Manuscript in preparation.

Scheme 3. C≡C Triple Bond Formation Caused by Recombination Events during the Gilch Synthesis of PPV



the CHX–CHX motif formed, a so-called TBB defect results (Scheme 2).

According to the reaction mechanism shown in Scheme 1, however, inverse monomer addition is not the only source of C≡C triple bonds: as the growing chains cannot lose their radical character via disproportionation, recombination of two radical chain ends is the only regular termination pathway accessible. Moreover, because recombination is most likely to occur between two CHX-centered radicals, a second type of C≡C triple-bond defect results after 2-fold dehydrohalogenation of the intermediately formed CHX–CHX moiety (Scheme 3): In contrast to the C≡C triple bonds caused by head–head monomer addition (Scheme 2), those formed following the recombination pathway are not necessarily located next to a saturated CH<sub>2</sub>–CH<sub>2</sub> moiety. Nevertheless, recombination events do not alter the 1:1 ratio of C≡C triple bonds and CH<sub>2</sub>–CH<sub>2</sub> single bonds in the PPVs because each recombination step causing a triple bond has a radical formation step  $2 \times 2 \rightarrow 3^*$  in its prehistory, which is the source of the associated CH<sub>2</sub>–CH<sub>2</sub> single bond. Moreover, because all growing chains are macro-diradicals, recombination always leads back to another macro-diradical, which continues chain growth further. Hence, not only inverse monomer placements but recombination events as well are expected to contribute to the formation of CH<sub>2</sub>–CH<sub>2</sub> single bond and C≡C triple bond defects, and hence to their CHX–CHX “precursor defects”, too.

Awareness of the mentioned dual mechanism of CHX–CHX defect generation might be of considerable relevance for future work dealing with the improvement of PPV-based devices because in this paper we will demonstrate that the already-mentioned halide defects are the key parameter determining the performance and lifetime of Gilch-PPV-based OLEDs. Essentially, it is argued that halide defects are rather significant than the “classic” C≡C triple bond or CH<sub>2</sub>–CH<sub>2</sub> single bond defects. Also, residual benzyl halide groups as shown in Figure 1 do not represent critical defects because they are simply highly unlikely because chain growth leading to **4\*** and subsequent macromolecular dehydrohalogenation

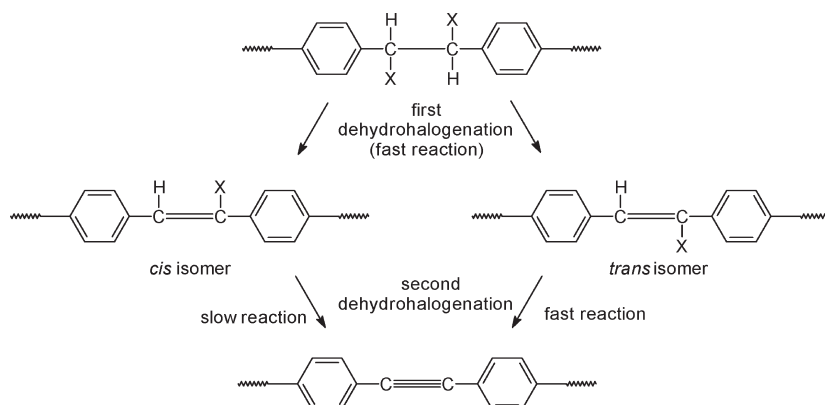
**4\*** → **5\*** are of similar rate and thus proceed (and complete) nearly simultaneously. Therefore, there is no reason why CHX–CH<sub>2</sub> units might survive the reaction conditions by more than a few minutes presumed there is a sufficiently high excess of KO<sup>*t*</sup>Bu available in the reaction mixture (as is usually the case). This statement is in full agreement with in situ NMR and UV–vis spectroscopic studies.<sup>19–21,23</sup> Instead, there must be a different reason for “persistent” halides in Gilch PPVs. Chain termini, also sometimes assumed to be the source of halide contaminations, can be ignored in this context—keeping in mind the tremendously high chain lengths realized in Gilch polymerizations.

The question why long-term persistent halides are residing in Gilch PPVs can be answered by the aforementioned observation that there is always a certain amount of cis-configured repeating units present in the otherwise trans-configured PPV chains. This allows concluding that dehydrohalogenation of the CHX–CH<sub>2</sub> intermediate is not completely trans-selective. Thus, it is reasonable to assume that also the first dehydrohalogenation of the CHX–CHX defects is not completely trans-selective either. On the contrary, because of the bulkiness of the halide substituent of the CH=CX intermediate, an even higher amount of cis-configured vinylenic moieties is expected in this latter case (Scheme 4). This explains why there are persistent halides in the finally obtained PPVs: although trans-configured CH=CX moieties undergo their second dehydrohalogenation to give C≡C triple bonds very rapidly, their cis-configured counterparts do not. Here, dehydrohalogenation is kinetically hindered and consequently, the cis-configured CH=CX motifs survive even the basic reaction conditions of Gilch syntheses for quite a long time. Only very slowly, upon prolonged treatment under reaction conditions and possibly accelerated by heating, this final dehydrohalogenation of cis-configured CH=CX groups proceeds as well, either via intermediate cis–trans isomerization or via an alternative reaction mechanism.

Localization of the remaining halides at *cis*-configured CH=CX motifs are considered to be also the reason why it was impossible to find characteristic absorptions of



Scheme 4. Constitution of Persistent Halide Defects in Gilch-Synthesized PPV



$\text{CH}_2\text{—CHX}$  benzyl halides in the NMR spectra of typical Gilch PPVs.<sup>4</sup> On this chain of evidence, it is reasonable to assume that persistent *cis*-configured  $\text{CH}=\text{CX}$  moieties (sometimes called “vinyl halide defects” in the following) might be essential for OLED lifetimes and performance.

## Results

**Optimized Dehydrohalogenation.** The chemical structure of  $\text{OC}_8\text{C}_8$ , the soluble PPV derivative used in this work, is shown in the inset of Figure 2. Like the well-known PPVs  $\text{OC}_1\text{C}_{10}$  and poly[*p*-(2-methoxy-5-(2-ethylhexyloxy)phenylene-vinylene)] (MEH-PPV), it is substituted by two alkoxy side chains. To study the influence of the mentioned halide defects on the performance of PPV-based OLEDs, we Gilch-polymerized  $\text{OC}_8\text{C}_8$  with various synthesis times without changing the experimental conditions otherwise. Hereafter, the resulting polymers are referred to as “*x* h PPV” or “*x* h material” and so on, where *x* denotes the synthesis time. The range of 1.5–96 h covers and extends the typical synthesis times of up to 24 h for the Gilch polymerization of PPVs.<sup>8,26</sup> The used monomer features bromine leaving groups and the amount of residual bromine in the resulting polymer is determined by ion chromatography and elemental analysis. Table 1 summarizes the bromine content for polymers with various synthesis times. As expected from the mechanistic considerations in the previous section, the bromine content decreases with increasing synthesis time: The content of 0.39 wt % of bromine for a synthesis time of 1.5 h is reduced by almost an order of magnitude to 0.048 wt % for the 50 h polymer. Also given in Table 1 is the percentage of repeat units affected by the defects, which can be calculated by taking into account the molar masses of bromine and of the regular  $\text{OC}_8\text{C}_8$  repeat units.

**OLED Characteristics.** The PPVs with different synthesis times are employed in single-layer OLEDs with poly(styrenesulfonate)-doped poly(3,4-ethylenedioxythiophene) (PEDOT:PSS) on indium tin oxide (ITO) as anode, calcium as cathode, and a thickness of the active PPV layer of 130 nm. A typical electroluminescence

spectrum is depicted in Figure 2. It features a broad maximum around 590 nm like other dialkoxy PPVs such as MEH-PPV and  $\text{OC}_1\text{C}_{10}$ .<sup>1,26,27</sup> The emitted light is orange in color and has CIE color coordinates of  $x = 0.57$  and  $y = 0.43$ . This emission characteristic does not change with varying synthesis time, i.e., it is independent of the content of bromide defects.

The current–voltage and luminance–voltage characteristics of the  $\text{OC}_8\text{C}_8$ -based OLEDs for different synthesis times of the polymer are shown in Figure 3. The applied voltage is corrected by the built-in voltage  $U_{\text{bi}} = 2.3$  V estimated from the difference of the work functions of the electrode materials, which are 5.2 eV for PEDOT:PSS and 2.9 eV for calcium.<sup>28,29</sup> The current density achievable at the same voltage increases for longer synthesis times of the polymer. The current density is up to three times higher for the 96 h polymer in comparison to the 3 h material. The same trend, but even more pronounced can be seen in the luminance–voltage characteristics: A longer synthesis time in the Gilch polymerization, i.e., a lower amount of bromide defects, leads to a much higher luminance of the resulting OLEDs. There is a difference of one to 2 orders of magnitude between 3 h and 96 h synthesis time. Because the luminance increases more strongly upon lowering the bromide content than the current density does, it is also instructive to examine the luminance efficiency. As can be seen in Figure 4, the luminance efficiency is also strongly increased by extending the synthesis time: it is up to an order of magnitude higher for the 96 h  $\text{OC}_8\text{C}_8$  than for the 3 h material. Concomitantly, the emission color does not change upon a varied synthesis time. Table 1 summarizes the current density at an internal voltage of 9.7 V and the maximum luminance efficiency for the OLEDs based on PPVs with different synthesis times, i.e., different bromide content. The increases in current density, luminance, and luminance efficiency are most pronounced in the regime of relatively small synthesis times and tend to saturate for higher synthesis times. Extending the

(26) Spreitzer, H.; Becker, H.; Kluge, E.; Kreuder, W.; Schenk, H.; Demandt, R.; Schoo, H. *Adv. Mater.* **1998**, *10*, 1340.

(27) Braun, D.; Staring, E. G. J.; Demandt, R. C. J. E.; Rikken, G. L. J.; Kessener, Y. A. R. R.; Venhuizen, A. H. J. *Synth. Met.* **1994**, *66*, 75.

(28) Brown, T. M.; Kim, J. S.; Friend, R. H.; Cacialli, F.; Daik, R.; Feast, W. J. *Appl. Phys. Lett.* **1999**, *75*, 1679.

(29) Lide, D. R. *CRC Handbook of Chemistry and Physics*; CRC Press: Boca Raton, FL, 1996.

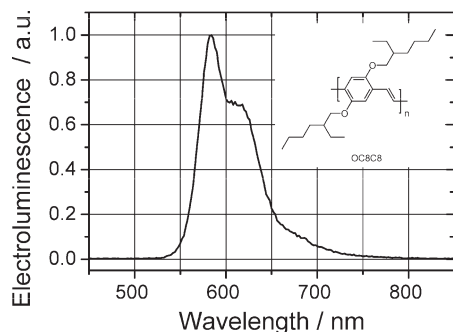


**Figure 2.** Electroluminescence spectrum of an OLED based on poly-*p*-(2,5-di(2-ethylhexyloxy)phenylene-vinylene) (OC<sub>8</sub>C<sub>8</sub>). The inset shows the chemical structure of OC<sub>8</sub>C<sub>8</sub>.

**Table 1.** Defect Content of OC<sub>8</sub>C<sub>8</sub> PPVs with Various Synthesis Times and Performance and Lifetime Data of the Corresponding OLEDs

synthesis time (h)	Br content (wt %)	bromide defects (% of repeat units)	<i>f</i> @ 9.7 V internal bias (mA/cm <sup>2</sup> )	max. luminance efficiency (cd/A)	<i>t</i> <sub>1/2</sub> (h) at 50 mA/cm <sup>2</sup>
1.5	0.39	1.8			
3	0.27	1.2	197 ± 41	0.1 ± 0.05	~1
6	0.086	0.4	449 ± 21	0.21 ± 0.03	~1
50	0.048	0.2	659 ± 102	0.49 ± 0.19	90–183
96			623 ± 37	0.67 ± 0.17	206–307

synthesis time from 50 to 96 h, the differences in the characteristics are already within the experimental error.

**OLED Lifetime.** Figure 5 depicts the lifetime measurements at a constant current density of 50 mA/cm<sup>2</sup> for the OLEDs based on OC<sub>8</sub>C<sub>8</sub> with different synthesis times. They show the typical qualitative behavior of OLEDs operated under constant current conditions.<sup>30–34</sup> The voltage required to drive the constant current increases and the luminance decreases over time. Both effects are mitigated for longer synthesis times of the polymer. The time it takes the luminance to drop to almost zero is already extended to approximately 100 h once the synthesis time is increased from 3 to 6 h. However, the lifetimes *t*<sub>1/2</sub>, which are defined as the times when the luminance has reached half of its initial value,<sup>35</sup> are alike for both devices because of the fast initial drop in the luminance. This pronounced initial drop of the luminance can be attenuated by extending the synthesis time further to 50 h. The step from 6 to 50 h thus displays the most pronounced stabilization of the OLEDs per synthesis time, where the lifetime *t*<sub>1/2</sub> is increased from mere hours to approximately 90–180 h. Further increasing the synthesis time of OC<sub>8</sub>C<sub>8</sub> to 96 h and hence decreasing the amount of bromide defects does not hamper the fatigue of the OLED performance as efficient; the stabilization tends to

saturate. Anyhow, *t*<sub>1/2</sub> extends to approximately 200–300 h. All measured lifetimes are summarized in Table 1.

Compared to a lifetime determination at equal initial current, its determination at equal initial brightness is more relevant for OLED applications. In this respect, a constant current density of 50 mA/cm<sup>2</sup> corresponds to an initial luminance of about 270 and 35 cd/m<sup>2</sup> for the OLEDs based on the 96 and 3 h material, respectively. To achieve equal initial luminance, the OLED based on the PPV with the shortest synthesis time has to be driven at higher current densities than devices based on longer synthesized materials, implying a stronger electrical stress for the former. As a consequence, the difference in the long term stability of the employed polymers is found to be even more pronounced (not shown) if compared to the lifetime spreading obtained at equal initial current.

**Charge Carrier Transport.** To study the influence of the bromide defect on the charge carrier transport, the charge carrier mobilities  $\mu$  for the two polymers with the shortest and longest synthesis time of 3 h and 96 h, respectively, are determined by optical time-of-flight measurements.<sup>36</sup> A typical hole current transient is shown in the inset of Figure 6. It features a well-defined drop in the transient current, which marks the transit time  $\tau$  of the traversing charge carrier package, and exhibits only slightly dispersive features. The hole mobility is calculated from the transit time as a function of the electric-field strength *E* and is plotted in Figure 6 for the 3 h and 96 h PPV. It can be seen that the hole mobilities are not affected by the different amount of bromide defects in those two materials.

The electric-field dependence of the charge carrier mobility in amorphous organic semiconductors is described by<sup>37</sup>

$$\mu = \mu^* \exp(\gamma \sqrt{E}) \quad (1)$$

with the zero field mobility  $\mu^*$  and a material constant  $\gamma$ . A fit of eq 1 to the data presented in Figure 6 yields  $\mu^* = 4.4 \times 10^{-5}$  cm<sup>2</sup>/(Vs) and  $\gamma = 1.5 \times 10^{-3}$  (cm/V)<sup>1/2</sup>.

In principle, the time-of-flight technique allows for the determination of both the hole and electron mobility.<sup>36</sup> However, electron transport in PPVs is governed by the capture of electrons in deep traps, impeding the determination of the effective charge carrier mobility for electrons by time-of-flight measurements.<sup>38–40</sup> To nevertheless gain information on the influence of the bromide defects on electron transport, we studied the current–voltage characteristics of electron-only devices.<sup>39</sup> For this, a 200-nm-thick layer of the polymer is sandwiched between calcium electrodes that facilitate easy electron injection, but block the injection of holes into the

(30) Aziz, H.; Popovic, Z. D.; Hu, N.-X.; Hor, A.-M.; Xu, G. *Science* **1999**, 283, 1900.

(31) Popovic, Z. D.; Xie, S.; Hu, N.; Hor, A.; Fork, D.; Anderson, G.; Tripp, C. *Thin Solid Films* **2000**, 363, 6.

(32) Silverstre, G. C. M.; Johnson, M. T.; Giraldo, A.; Shannon, J. M. *Appl. Phys. Lett.* **2001**, 78, 1619.

(33) Cusumano, P.; Buttitta, F.; Di Cristofalo, A.; Cali, C. *Synth. Met.* **2003**, 139, 657.

(34) Aziz, H.; Popovic, Z. D. *Chem. Mater.* **2004**, 16, 4522.

(35) Dodabalapur, A. *Solid State Commun.* **1997**, 102, 259.

(36) Borsenberger, P. M.; Weiss, D. *Organic Photoreceptors for Xerography*; Eastman Kodak: Rochester, NY, 1998.

(37) Bässler, H. *Phys. Status Solidi B* **1993**, 175, 15.

(38) Antoniadis, H.; Abkowitz, M. A.; Hsieh, B. R. *Appl. Phys. Lett.* **1994**, 65, 2030.

(39) Blom, P. W. M.; de Jong, M. J. M.; Vleggaar, J. J. M. *Appl. Phys. Lett.* **1996**, 68, 308.

(40) Mandoc, M. M.; de Boer, B.; Blom, P. W. M. *Phys. Rev. B* **2006**, 73, 155205.

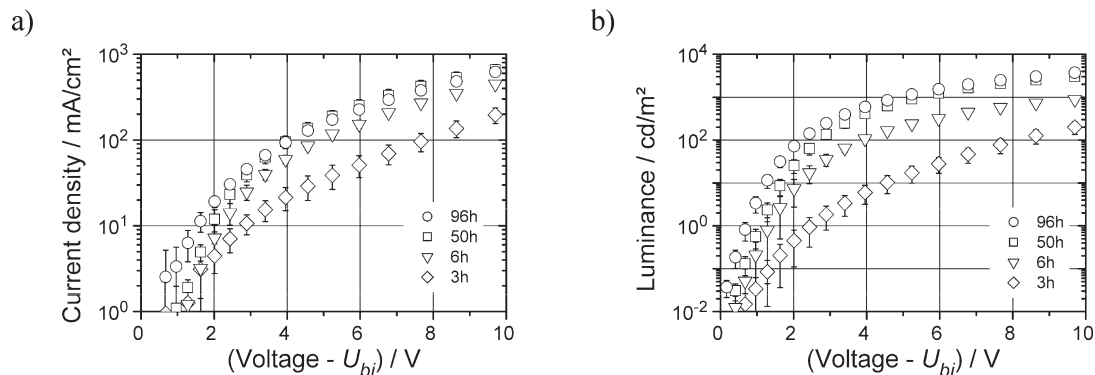


**Figure 3.** (a) Current–voltage and (b) luminance–voltage characteristics of OC<sub>8</sub>C<sub>8</sub>-based OLEDs for different synthesis times of the polymer, i.e., for different bromide contents.

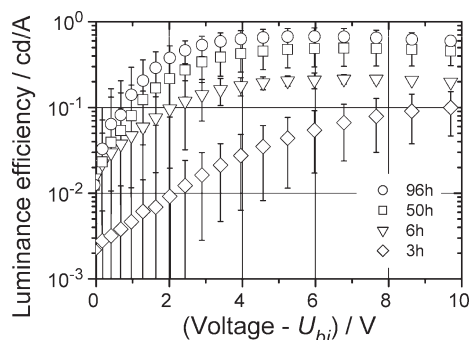


**Figure 4.** Luminance efficiency vs voltage for different synthesis times of the polymer, i.e., for different bromide contents.

polymer. Thus, only electrons can contribute to the resulting current, which is shown in Figure 7. Because the same material is used as anode and cathode in those devices, no built-in voltage drops across the polymer layer. In the low voltage regime, the current density is dominated by leakage currents. For higher voltages, where the current–voltage characteristics are governed by the conduction through the bulk material of the polymer, the devices based on the 96 h material exhibit a higher current density than the devices made from 3 h PPV; the current density increases up to an order of a magnitude by extending the synthesis time of the polymer from 3 to 96 h.

Apparently, the current densities obtained for the electron-only devices are far below those of the bipolar OLEDs presented in Figure 3 a. For similar electric field strengths  $E = U/d$ , where  $U$  is the internal voltage drop, the current density is reduced by at most 5 orders of magnitude between the bipolar OLEDs and the electron-only devices. Thus, in view of the TOF result and assuming that Ca forms a sufficiently good contact with OC<sub>8</sub>C<sub>8</sub>–PPV for electron injection (no injection limitation), a substantial smaller electron mobility compared to those of holes is the most likely explanation for the attenuated current density observed in electron only devices if compared to bipolar devices.

### Discussion

**Significance of the Vinyl Halide Defect.** The results summarized in Table 1 confirm that a considerable amount of halogen groups can remain uneliminated when

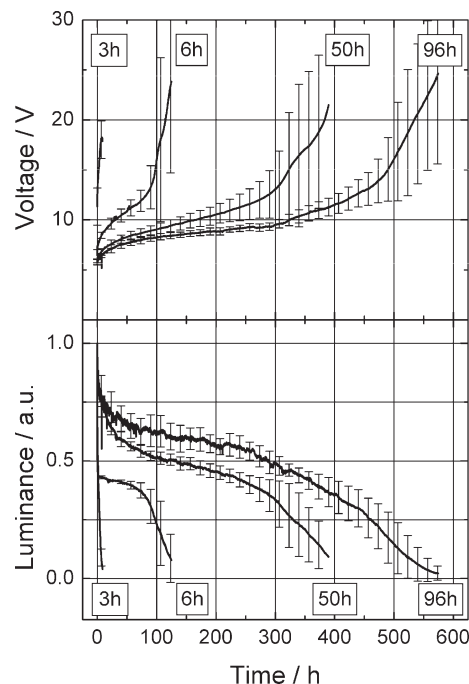


**Figure 5.** Lifetime measurements at a constant current density of 50 mA/cm<sup>2</sup> for OLEDs based on OC<sub>8</sub>C<sub>8</sub> with different synthesis times, where a higher synthesis time corresponds to a lower amount of halide defects. Top: Driving voltage vs time. Bottom: Normalized luminance vs time. The luminance is normalized to its initial value.

a dialkoxy substituted PPV is synthesized via the Gilch route under typical experimental conditions. The amount of bromide defects detected for short synthesis times is on the same order of magnitude as the few values reported in the literature.<sup>9,16</sup> Figure 8 depicts the correlation between the synthesis time of the polymer and the amount of uneliminated halogen groups. Extending the synthesis time proves to be a viable way of increasing the degree of dehydrohalogenation and thus decreasing the amount of remaining halide defects. The highest amount of residual bromine is detected for the shortest synthesis time of 1.5 h, where 1.8% of the repeat units are affected by the bromide defect. This defect content translates into an average distance of 57 repeat units between two bromide defects in the polymer chain, which is far above the effective conjugation length of typically a few repeat units.<sup>7</sup> Therefore, even if the halide defects interrupted the

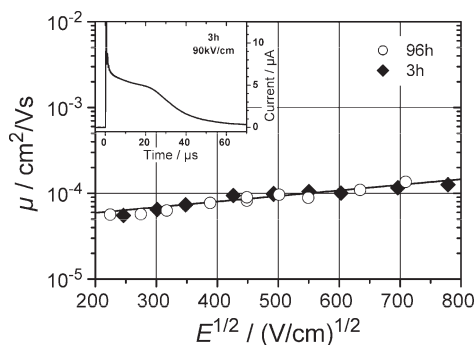


**Figure 6.** Hole mobility  $\mu$  in  $\text{OC}_8\text{C}_8$  vs the square root of the electric field strength  $E$  for different synthesis times of the polymer, as indicated in the legend. The straight line is a fit of eq 1 to the data. The inset shows a typical time-of-flight hole current transient.

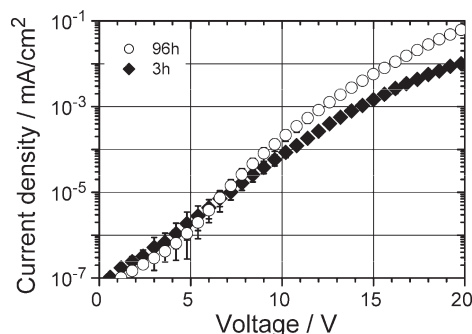


**Figure 7.** Current density as a function of the applied voltage of  $\text{OC}_8\text{C}_8$  electron-only devices for different synthesis times of the polymer.

$\pi$ -conjugation along the PPV backbones, such interruption cannot be expected to influence the emission characteristics of the polymer, in accordance with the experimental results: Despite the different degree of dehydrohalogenation the emission color does not vary between the polymers prepared with different synthesis times. Be aware that it is even not obvious whether the relevant vinyl halide defects affect the conjugation at all even so the benzyl halide defects definitively would do.

Figure 8 also illustrates the effect of the halide defect on the lifetime of the PPV-based OLEDs. Because increasing the synthesis time does not change the amount of TBB defects, the presented results can be pinpointed to the halide defect, whereas the influence of varying TBB contents can be excluded. It is important to note how the bromine content correlates with the lifetime of the OLEDs: The decrease in the amount of bromide defects from 1.2% affected repeat units to 0.4% upon increasing the synthesis time from 3 to 6 h does not show as much an effect on the lifetime as the further decrease to 0.2% upon increasing the synthesis time to 50 h. This illustrates the significance of an incomplete dehydrohalogenation for the lifetime of PPV-based OLEDs, even if just fractions of a percent of the repeat units are affected by the halide defect and demonstrates that even small changes in the amount of remaining halide have a major impact on the lifetime of the devices. The same holds for the luminance efficiency of the OLEDs summarized in Table 1.

The lifetime and efficiency results imply that the halide defect has to be considered when different synthesis

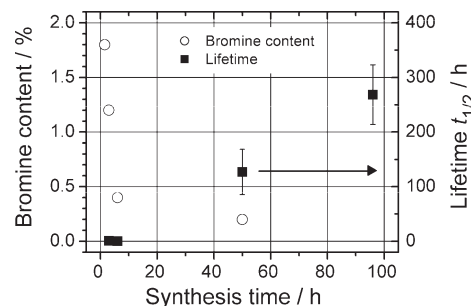


**Figure 8.** Bromine content and lifetime  $t_{1/2}$  vs the synthesis time of the polymer  $\text{OC}_8\text{C}_8$ . The bromine content is given as the amount of repeat units affected by the bromide defect.

conditions or different polymers are screened, even if the defect concentration is too low to be detected by routine NMR characterization. Furthermore, they cast doubt on the sole focus that is given to TBB defects in Gilch-polymerized PPVs. It cannot a priori be assumed that the dehydrohalogenation achieved during the Gilch synthesis is sufficient to exclude the impact of halide defects, when e.g. the correlation between the amount of TBB defects and the lifetime is studied.<sup>10</sup>

It can be seen from the device characteristics depicted in Figures 3 and 4 and from the lifetime measurements shown in Figure 5 that the decrease in halide defects by extending the synthesis time has a strong impact on the OLED performance up to synthesis times of 50 h. Further increasing the synthesis time shows no effect for the OLED characteristics of fresh devices and a comparatively moderate improvement in the long time stability under electrical stress. Hence, for the experimental conditions of the Gilch synthesis of  $\text{OC}_8\text{C}_8$  employed in this work, a synthesis time of a few days is required to render the perturbing impact of the bromide defect on the OLED performance negligible.

**Performance of  $\text{OC}_8\text{C}_8$  PPV-based OLEDs.** Even for the longest synthesis time of 96 h and concurrently the lowest amount of bromine defects, the luminance efficiency of the  $\text{OC}_8\text{C}_8$  OLEDs is rather low. A luminance of  $100 \text{ cd/m}^2$  is achieved at an external bias of 4.5 V and the luminance efficiency of the devices is only about  $0.4 \text{ cd/A}$  when operated at this point. In comparison, the well-known PPV derivative  $\text{OC}_1\text{C}_{10}$  reaches  $100 \text{ cd/m}^2$  at just 2.7 V external bias with a luminance efficiency of  $2.1 \text{ cd/A}$  in a comparable device setup.<sup>26</sup> The reason for the moderate performance of  $\text{OC}_8\text{C}_8$  can be deduced from its high hole mobility. The zero field mobility  $\mu^* = 4.4 \times 10^{-5} \text{ cm}^2/(\text{Vs})$  of  $\text{OC}_8\text{C}_8$  is found to be 2 orders of magnitude higher than the zero field mobility of common PPV derivatives such as  $\text{OC}_1\text{C}_{10}$  and MEH-PPV, for which values of  $5 \times 10^{-7} \text{ cm}^2/(\text{Vs})$  and  $3 \times 10^{-7} \text{ cm}^2/(\text{Vs})$  have been reported, respectively.<sup>41,42</sup> The high mobility in  $\text{OC}_8\text{C}_8$  can be ascribed to the bulky, symmetric side chains, which lead to a smaller degree of disorder and thus a smaller degree of energetic disorder. On the one hand, this results in a higher mobility in the amorphous

(41) Blom, P. W. M.; de Jong, M. J. M.; van Munster, M. G. *Phys. Rev. B* **1997**, *55*, R656.

(42) Malliaras, G. G.; Salem, J. R.; Brock, P. J.; Scott, C. *Phys. Rev. B* **1998**, *58*, 13411.



polymer, as compared to the asymmetric side chains of OC<sub>1</sub>C<sub>10</sub> and MEH-PPV.<sup>43</sup> On the other hand, a reduced energetic disorder also favors exciton diffusion and thus increases their diffusion length, which results in an increased quenching region at the cathode and thus in reduced light output.<sup>44</sup> Be aware that because of the unbalanced charge-carrier mobilities in PPVs, the emission region is supposed to be located near the cathode, rendering quenching effects important.<sup>45</sup>

**Proposed Degradation Mechanism due to Halide Defects.** The effect of the bromide defect on the OLED characteristics observed in Figures 3 and 4 is to decrease the current density, luminance, and luminance efficiency at given voltage. However, the differences in device performance, especially in the  $I$ - $V$  characteristics of bipolar devices, need to be seen in view of the determined variations in the charge-carrier transport properties discussed above. This comparison will give a clear hint how the residual bromine might impede the OLED operation.

The current driven through a PPV-based OLED is limited by the bulk charge-carrier transport, if suitable contact materials like PEDOT:PSS and calcium provide ohmic injection of charge carriers.<sup>39</sup> The resulting bipolar bulk-limited current depends on the strength of the charge-carrier recombination and space-charge effects. Considering a finite bimolecular recombination coefficient  $B$ , and a trap free system, the current density  $j$  can be analyzed following the work of Parmenter et al. who calculated the two-carrier SCLC for insulators to be<sup>46,47</sup>

$$j = \frac{9}{8} \varepsilon_r \varepsilon_0 \mu_{\text{eff}} \frac{U^2}{d^3} \quad (2)$$

with the relative permittivity  $\varepsilon_r$ , the dielectric constant  $\varepsilon_0$ , the voltage  $U$ , the thickness of the organic layer  $d$ , and the effective mobility  $\mu_{\text{eff}}$  given by

$$\mu_{\text{eff}} = \frac{4}{9} \mu_r v_e v_h \left[ \frac{\Gamma(\frac{3}{2} v_e + \frac{3}{2} v_h)}{\Gamma(\frac{3}{2} v_e) \Gamma(\frac{3}{2} v_h)} \right]^2 \left[ \frac{\Gamma(v_e) \Gamma(v_h)}{\Gamma(v_e + v_h)} \right] \quad (3)$$

with  $v_e = \mu_e/\mu_r$ ,  $v_h = \mu_h/\mu_r$ , and  $\mu_r = \varepsilon_r \varepsilon_0 B / (2e)$ , where  $e$  is the elementary charge and  $\mu_e$  and  $\mu_h$  are the charge carrier mobilities for electrons and holes, respectively.  $\Gamma(x)$  is the Euler gamma function. Because charge carrier recombination in PPV-based derivatives is of the Langevin type, the charge carrier recombination coefficient is given as<sup>48,49</sup>

$$B = \frac{e(\mu_e + \mu_h)}{\varepsilon_r \varepsilon_0} \quad (4)$$

and  $v_e$ ,  $v_h$ , and  $\mu_r$  can be reformulated to  $v_e = 2 \mu_e / \mu_e(\mu_e + \mu_h)$ ,  $v_h = 2 \mu_h / (\mu_e + \mu_h)$  and  $\mu_r = (\mu_e + \mu_h) / 2$ . Because it was shown by the presented TOF measurements and the  $I$ - $V$  characteristics of bipolar and electron-only devices that the electron mobility is substantially lower than the hole mobility, the effective mobility  $\mu_{\text{eff}}$  can be expanded around  $\mu_e = 0$ . In the first-order approximation, eq 3 simplifies to

$$\mu_{\text{eff}} \approx \mu_h \left( 1 + 3 \frac{\mu_e}{\mu_h} \right) \quad (5)$$

From eq 5, it can be concluded that the determined effective mobility is essentially given by the hole mobility, as long as the electron mobility is assumed to be orders of magnitudes smaller than  $\mu_h$ .

The above estimation indicates how a variation of weak electron mobility may influence the effective mobility and thus the current density in a bipolar device. Since the electron mobility of the PPV - regardless of the bromine content - is supposed to be far below the one of holes (approximately 3 orders of magnitude), the effective mobility will not essentially differ from the hole mobility even for a change of 1 order of magnitude in  $\mu_e$  (see Figure 7). In addition, no variation in  $\mu_h$  could be detected via TOF for the different PPVs investigated and thus an unchanged bipolar  $I$ - $V$  characteristic is expected, contradicting the experimental observation. It is hence impossible to explain the substantial increase in the current density in bipolar devices upon increased synthesis time by charge-carrier transport phenomena alone and this conclusion does not change, even when substantial trapping of electrons is considered.

One essential drawback of the above model is that it assumes ohmic contacts but lacks the description of a hampered hole or electron injection or ejection at the anode or cathode, respectively. This indicates that instead of electron transport properties of the bulk, the contacts might predominantly determine the variation in the bipolar  $I$ - $V$  characteristics upon changed synthesis time. In turn, it cannot be excluded that besides a change in electron transport properties, a change in the contact formation prevails in the different electron-only devices, explaining the current variation.

A consequence of the reduced current density in bipolar devices comprising PPVs rich in vinyl bromide defects is a smaller number of formed excitons and thus less light output, in accordance with the experimental results. Even so, this does not explain per se why also the luminance efficiency is reduced. However, there is evidence that halogens can act as effective quenching centers in PPVs, which makes the decrease in luminance efficiency for higher contents of the bromide defect understandable.<sup>50</sup>

In view of the above considerations, it is possible to propose a mechanism for the observed differences in the performance of devices based on the 3 and the 96 h

(43) Martens, H. C. F.; Blom, P. W. M.; Schoo, H. F. M. *Phys. Rev. B* **2000**, *61*, 7489.

(44) Blom, P. W. M.; Martens, H. C. F.; Schoo, H. E. M.; Vissenberg, M. C. J. M.; Huijberts, J. N. *Synth. Met.* **2001**, *122*, 95.

(45) Neumann, F.; Genenko, Y. A.; Schmechel, R.; von Seggern, H. *Synth. Met.* **2005**, *150*, 291.

(46) Parmenter, R. H.; Ruppel, W. J. *Appl. Phys.* **1959**, *30*, 1548.

(47) Rosenberg, L. M.; Lampert, M. A. *J. Appl. Phys.* **1970**, *41*, 508.

(48) Langevin, P. *Ann. Chim. Phys.* **1903**, *28*, 289.

(49) Blom, P. W. M.; Vissenberg, M. C. J. M. *Mater. Sci. Eng., R* **2000**, *73*, 53.

(50) Hamer, P. J.; Pichler, K.; Harrison, M. G.; Friend, R. H.; Ratier, B.; Moliton, A.; Moratti, S. C.; Holmes, A. B. *Philos. Mag. B* **1996**, *73*, 367.

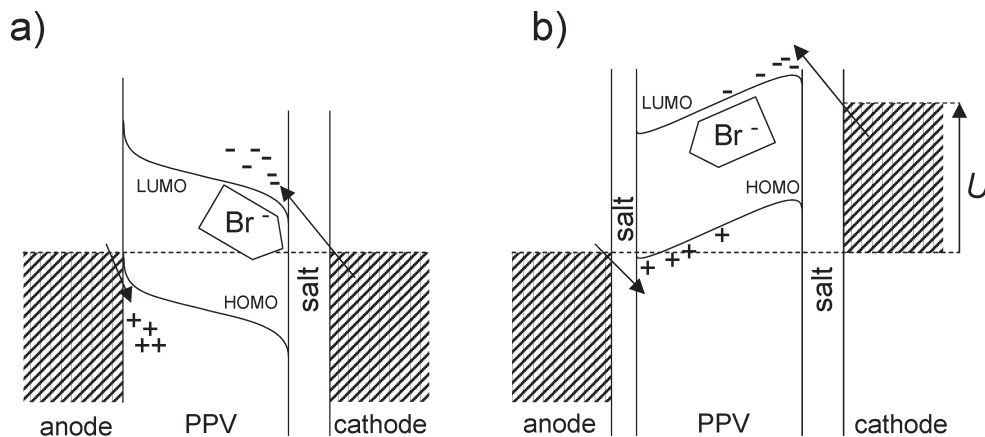


**Figure 9.** Schematic band diagram of an OLED rich on bromine at (a) zero bias and (b) strong forward bias. The two examples illustrate the proposed degradation mechanism for a fresh device and the suggested mechanism leading to the device fatigue, respectively.

polymer. The following considerations are concomitantly illustrated in Figure 9. Contacting the employed PPVs to Ca leads to diffusion of electrons from the metal into the organic semiconductor to establish thermal equilibrium (Figure 9a). The penetration of negative charges into the PPV is finally stopped by an emerging field driving the charges back to the cathode. As a consequence, a negative charge-carrier reservoir is established in the PPV in the vicinity of the Ca contact. However, a halogen atom covalently bound to a carbon can be eliminated as a halogen anion upon capture of an excess electron, leaving behind a radical on the polymer.<sup>17</sup> This suggests on the one hand that the halide defect acts like an electron trap removing electrons from the transport levels of the polymer. On the other hand, the resulting halogen anion will be driven to the contact by the electric field, where it can react with the contact material. In our case, the bromine might damage the Ca contact by forming a calcium bromide interlayer, thus impeding the electron injection (or the hole ejection).

Analogously, the rapid fatigue of OLEDs with a high amount of bromine is explainable. Again it is assumed that the halide defect acts as an electron trap. During device operation, electrons are transported through the organic layer, thus initiating the suggested reaction deeper in the organic layer. At high forward bias ( $U > U_{bi}$ ), the halogen anions will drift toward the ITO anode, forming indium bromide and/or tin bromide. Again, the injection (or ejection) is impeded, this time the injection of holes (ejection of electrons). One consequence of the proposed mechanism is that the spatial distribution of bromine should change during electrical stressing of the OLED. In future work, secondary ion mass spectrometry (SIMS) will be employed to prove this hypothesis.

### Conclusions

An incomplete dehydrohalogenation during the Gilch synthesis of PPV most likely leads to vinyl halide defects in the resulting polymer. The amount of repeat units affected by this defect is in the order of 1% for typical experimental conditions and can be reduced by increasing the synthesis time. The halide defect shows a pronounced

negative influence on the performance of PPV-based OLEDs, such as decreased luminance efficiency. Even more interestingly, the defect limits the OLED lifetime, even if just fractions of a percent of the repeat units contain uneliminated halides. It cannot a priori be assumed that the degree of dehydrohalogenation achieved during the Gilch polymerization of a PPV is sufficient to render the influence of the halide defect negligible. Therefore, it is mandatory to take into account the effect of a possibly varying content of the halide defect, when, for example, the influence of a varying amount of TBB on OLED lifetime is studied.

The negative impact of the halide defect on the performance of fresh devices can be attributed to two reasons: The halide defect seems on the one hand to constitute an electron trap, thus hindering the electron transport, and on the other hand to act as a luminescence quencher, thus further reducing the light output of the OLEDs. We propose that the halogen can be dissociated as an anion after capture of an excess electron and is consequently driven by the electric field to the cathode, where it damages the cathode by forming a salt. This impedes the performance of fresh OLEDs rich on halide defects. For the rapid failure of PPV-based OLEDs with a high amount of the defect, the ITO anode is affected by forming indium and/or tin halide.

### Experimental Section

**Synthesis.** All chemicals and solvents were purchased from Acros, Aldrich, and Strem Chemical Co. General procedures for drying the solvents, monomer synthesis, and polymer synthesis were as described recently.<sup>18–21</sup> Characterization of the monomers and polymers was done using NMR spectroscopy: NMR spectra were recorded using a Bruker ARX 300 NMR spectrometer working at 300 MHz (<sup>1</sup>H NMR) and 75 MHz (<sup>13</sup>C NMR), and on a Bruker DRX 500 NMR spectrometer working at 500 MHz (<sup>1</sup>H NMR) and 125 MHz (<sup>13</sup>C NMR). Elemental analyses were done by Malissa Analytische Laboratorien, Gummertsbach, Germany.

**Gilch Synthesis of OC<sub>8</sub>C<sub>8</sub> PPV (representative example).** 1,4-Bis(bromomethylene)-2,5-bis(2'-ethylhexyloxy)benzene (200 mg, 10 mmol L<sup>-1</sup>) is dissolved in very dry and oxygen-free tetrahydrofuran (THF). The solution is cooled to 0 °C. Under vigorous

stirring, 4 equiv of KOtBu, dissolved in dry and oxygen-free THF ( $3.3 \text{ mol L}^{-1}$ ), is added at once. The ice-bath is removed, and stirring at room temperature is continued over the indicated period of time (1.5, 3, 6, 50, and 96 h, respectively). Subsequently, the whole reaction mixture is poured into a 5-fold volume of methanol. The formed solid is collected and dried in a vacuum.

**Device Preparation.** Glass substrates coated with 100 nm ITO (Merck Display Technologies Ltd.) are photolithographically structured, ultrasonically cleaned in deionized water and acetone and are subjected to a UV ozone treatment. PEDOT:PSS dispersed in water (Baytron P VP AI 4083 formulation by H. C. Starck GmbH) is spin-coated on the substrates in air and baked out at  $110^\circ\text{C}$  for 5 min to form a 30-nm-thick film. Subsequently, OC<sub>8</sub>C<sub>8</sub> is spin-coated in a nitrogen glovebox from toluene solution (typically 0.7 wt %) to yield layers with 130 nm thickness. The samples are transferred to a vacuum chamber without exposure to ambient atmosphere to deposit 20 nm of calcium and 100 nm of aluminum by physical vapor deposition. The organic diodes are defined by the overlap of the ITO anode structure and the Ca/Al cathode strip and have an active area of  $10 \text{ mm}^2$ . The samples are transferred under vacuum to another nitrogen glovebox for characterization and lifetime measurements.

For the electron-only devices, 20 nm of calcium are deposited onto the ITO anode structure before the samples are transferred under vacuum to the nitrogen glovebox for spin-coating of the polymer. For time-of-flight samples, a semitransparent, 10-nm-thick Al layer is deposited on the ITO structure prior to the spin-coating of a polymer film with a thickness of a few micrometers, and in this case the devices are topped just with a 100-nm-thick Al electrode.

**Device Characterization.** All measurements are conducted under a nitrogen atmosphere. Current density–luminance–voltage characteristics of the OLEDs are measured in the dark with a HP 4155A parameter analyzer, employing silicon photodiodes for measuring the light output. CIE color coordinates and calibration data for luminance values are determined with a spot-photometer (Minolta CS-100). The EL spectrum is recorded with a Cary Eclipse spectrometer from Varian Inc. For lifetime measurements, the OLEDs are driven under constant current conditions at  $50 \text{ mA/cm}^2$ , while the applied voltage and the light output are detected as a function of the operation time of the device. A frequency-doubled Nd:YAG laser (532 nm) is used for the time-of-flight measurements; the experimental details of the time-of-flight setup are published elsewhere.<sup>51</sup>

**Acknowledgment.** The authors thank the Deutsche Forschungsgemeinschaft (German Research Foundation) for the financial support through the Collaborative Research Center SFB 595.

(51) Fleissner, A.; Schmid, H.; Melzer, C.; von Seggern, H. *Appl. Phys. Lett.* **2007**, *91*, 242103.